



## Tuning the properties of electrospun polylactide mats by ethanol treatment

Elizaveta R. Pavlova<sup>a,b</sup>, Dmitry V. Bagrov<sup>a,c</sup>, Kristina Z. Monakhova<sup>d</sup>, Alexey A. Piryazev<sup>b,e,f</sup>, Anastasia I. Sokolova<sup>a,c</sup>, Dimitri A. Ivanov<sup>b,e,f,g</sup>, Dmitry V. Klinov<sup>a,b,\*</sup>

<sup>a</sup> Federal Research and Clinical Center of Physical-Chemical Medicine of Federal Medical Biological Agency, Malaya Pirogovskaya Street 1a, 119435 Moscow, Russian Federation

<sup>b</sup> Moscow Institute of Physics and Technology, Institutskiy Per. 9, 141700 Dolgoprudny, Moscow Region, Russian Federation

<sup>c</sup> Lomonosov Moscow State University, Faculty of Biology, Department of Bioengineering, Leninskie Gory 1/12, 119991 Moscow, Russian Federation

<sup>d</sup> Enikolopov Institute of Synthetic Polymeric Materials of Russian Academy of Sciences, Profsoyuznaya Street 70, 117393 Moscow, Russian Federation

<sup>e</sup> Lomonosov Moscow State University, Faculty of Fundamental Physical and Chemical Engineering, Leninskie Gory 1/51, 119991 Moscow, Russian Federation

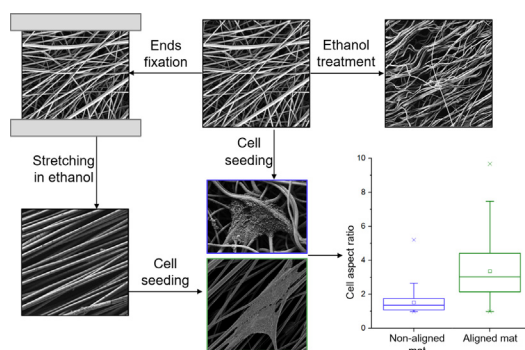
<sup>f</sup> Institute of Problems of Chemical Physics of Russian Academy of Sciences, Academician Semenov avenue 1, 142432 Chernogolovka, Moscow Region, Russian Federation

<sup>g</sup> Institut de Sciences des Matériaux de Mulhouse-IS2M, CNRS UMR 7361, F-68057 Mulhouse, France

### HIGHLIGHTS

- Ethanol treatment of electrospun PLA mats led to their shrinkage and fibers crimping without an increase of crystallinity
- Both free-ends and fixed-ends ethanol-treated PLA mats had a higher elongation at break than the non-treated ones
- Stretching of PLA mats in ethanol caused their high alignment while stretching in air led to fibers necking and poor alignment
- Ethanol-stretched PLA mats caused contact guidance of HaCaT human keratinocytes

### GRAPHICAL ABSTRACT



### ARTICLE INFO

#### Article history:

Received 14 June 2019

Received in revised form 18 July 2019

Accepted 19 July 2019

Available online 21 July 2019

#### Keywords:

Electrospinning

Shrinkage

Aligned mats

Contact guidance

### ABSTRACT

In the present work, we analyzed the changes in structure and mechanical properties of electrospun PLA mats induced by ethanol treatment. The amorphous PLA mats gained elasticity when immersed into ethanol (the elongation at break increased from  $\epsilon$ -50% in air to  $\epsilon$ -280% in ethanol) and partly retained it after drying ( $\epsilon$ -110%). At the nanoscale, the ethanol treatment caused crimping of the fibers without crystallinity increase. Stretching of the electrospun mats in ethanol caused high alignment of the fibers (geometrical orientation factor  $f = 0.92$ ) without the need for a special collector electrode such as a pair of blades, which yielded mats with geometrical orientation factor  $f = 0.71$ . The aligned mats prepared by stretching in ethanol caused contact guidance of HaCaT human keratinocytes and did not taint viability and proliferation rate of cells in comparison with the non-aligned ones. Our research demonstrates the tuning of electrospun mats properties by post-treatment without any modification of the chemical structure.

© 2019 The Author(s). Published by Elsevier Ltd. This is an open access article under the CC BY-NC-ND license (<http://creativecommons.org/licenses/by-nc-nd/4.0/>).

\* Corresponding author.

E-mail address: [dmitry.klinov@rcpcm.org](mailto:dmitry.klinov@rcpcm.org) (D.V. Klinov).

## 1. Introduction

Electrospinning is a method to fabricate nano- and micro-fibrous materials which can be used for cell culturing [1,2], tissue engineering scaffolds [3,4], gases and liquid filters [5,6], sorbents [7,8] and other applications [9,10]. The properties of electrospun mats can be tuned by various post-processing methods – heating, radiation or chemical treatment [11–13]. Among the diversity of post-processing methods, the simple ethanol treatment is of great interest. It can be used not only as a disinfection method for electrospun mats but also to modify the mat properties, including morphology, crystallinity, mechanical and biological properties.

Only a few papers describe structural changes in electrospun mats which occur upon their post-treatment with ethanol [14–18]. They focus on electrospun biodegradable polyesters – poly (lactic acid) (PLA) and its copolymers. Ethanol acts as a plasticizer for the on electrospun PLA mats and can modify fiber shape and size, physical properties and biocompatibility of mats. Firstly, the immersion of electrospun PLA mats into ethanol led to their shrinkage accompanied by fibers crimping [14,15]. Similar crimping was observed when the electrospun mats were heated [19,20]. The electrospun poly(L-lactide-co-ε-caprolactone) (PLCL) fibers became crimped when the operating temperature during incubation of electrospun mats in phosphate buffered saline (PBS) was higher than the polymer glass-transition temperature [16]. The fiber crimping was retained after the temperature decreased. Secondly, ethanol can modify crystallinity and, as a result, mechanical properties of electrospun PLA mats. The amorphous electrospun poly-L-lactide (PLLA) mats developed an amount of crystal phase up to 20% during an ethanol treatment at room temperature (RT) because of the plasticizing effect of ethanol, which enlarged the temperature window of the PLLA crystallization to RT [14]. The authors observed the crystallinity increase of fixed electrospun PLLA mats upon treatment in absolute ethanol, which occurred on the scale of a few hours and resulted in the formation of α-phase of PLLA. Liu and colleagues [15] noted that the residual stress of polymer chains during ethanol treatment could be converted either into increased crystallinity (in case of the electrospun mat fixation) or into shrinkage with the formation of crimped fibers (in case of the free-ends mats treatment).

Increased crystallinity caused an increase in Young's modulus, while the crimped fibers' structure was accompanied by the lower crystallinity and a higher yield strain. However, Chao and co-authors [21] reported about crystallinity increase of electrospun PLLA mats with crimped fibers prepared by heating or ethanol treatment. Finally, the ethanol-treated crimped electrospun fibers demonstrated promising biomechanical properties [15,16]. The crimped fibers imitated the morphology of collagen fibrils, which constitute the extracellular matrix (ECM) [22]. For example, electrospun PLCL crimped fibers provided good attachment and proliferation of bovine fibroblasts [16]. The proliferation rate of mouse fibroblasts on ethanol sterilized electrospun polycaprolactone (PCL) and PLCL mats was faster than on ethylene oxide treated ones [23], presumably, due to the crimped fibers' structure. Therefore, the potential applications of the discussed phenomena remain underestimated.

In the present work, we thoroughly analyzed several aspects of the treatment of electrospun PLA mats with ethanol (Fig. 1). We investigated the shrinkage kinetics and mechanical properties of ethanol-treated electrospun PLA mats with free and fixed ends. The usage PLA with a small fraction of D-isomer helped us to avoid crystallinity increase during ethanol treatment and a possible decrease of extensibility. We proposed a new method to obtain aligned fibers by stretching of electrospun PLA mats in ethanol. This method seemed simpler than the routine usage of a special collector electrode (a pair of blades) and provided higher alignment of the fibers. We demonstrated that the mats manufactured by our method induced cell elongation and can be used cell contact guidance studies.

## 2. Materials and methods

### 2.1. Electrospinning process

Electrospun mats were prepared using the Nanofiber Electrospinning Unit apparatus (China) from 100 mg/ml solution of polylactide (REC, Russia) in 1,1,1,3,3,3-hexafluoroisopropanol (P&M-Invest, Russia). We used PLA with the 4.5% fraction of D-isomer, according to the supplier. Two types of mats were obtained: non-aligned and aligned. The non-aligned mats were obtained on a polypropylene frame positioned

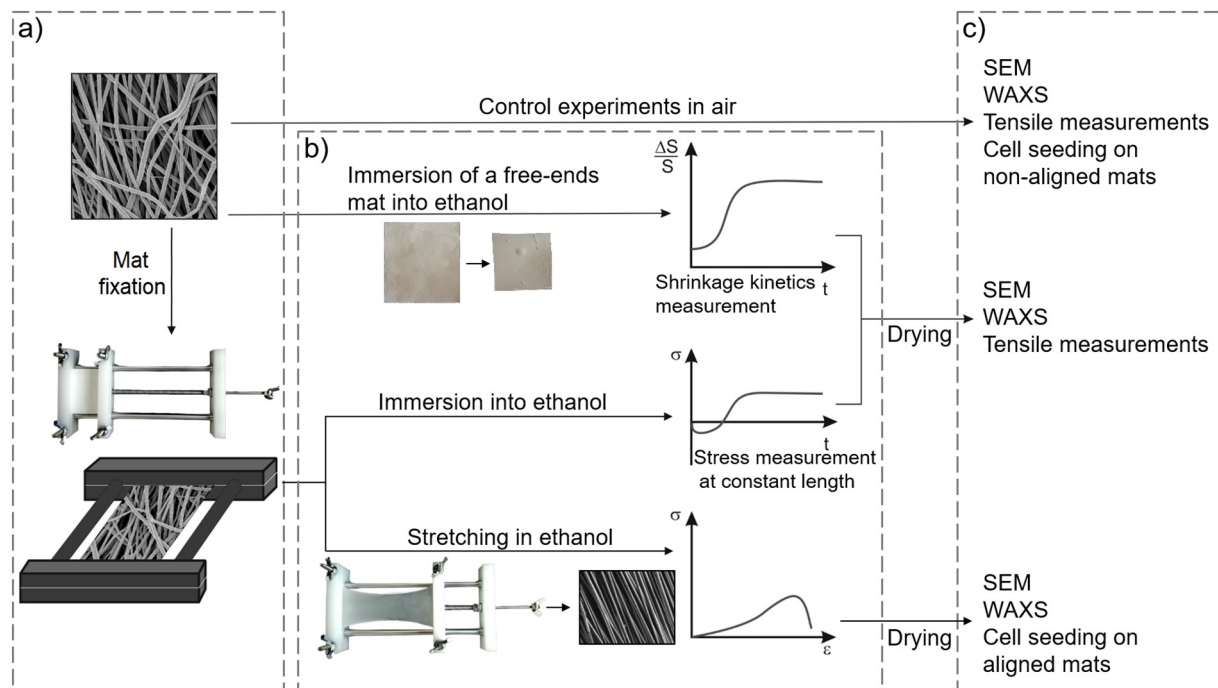


Fig. 1. The general scheme of experiments: a) electrospun PLA samples, b) types of ethanol treatment, c) characterization of the electrospun mats.

between two electrodes: the feeding syringe needle and a counter-electrode [24]. The aligned mats were produced using two parallel metal blades as the collector. The accelerating voltage and distance between the needle and the second electrode were 30 kV and 30 cm, respectively. The polymer solution was supplied at a rate of 1 ml/h, the inner diameter of the syringe needle was 0.7 mm. Also, high-aligned mats were obtained from the ordinary non-aligned electrospun mats by two times stretching them in ethanol. To obtain quantitative information on the extent of geometrical orientation of the fibers upon uniaxial stretching, we calculated the geometrical Herman orientation factor ( $f_g$ ) [25] as the  $P_2$  Legendre polynomial:

$$f_g = \frac{1}{2} \left( \frac{3 \int_0^{\frac{\pi}{2}} D(\alpha) \cos^2 \alpha \sin \alpha \, d\alpha}{\int_0^{\frac{\pi}{2}} D(\alpha) \sin \alpha \, d\alpha} - 1 \right), \quad (1)$$

where  $\alpha$  is an angle between fiber, as observed by SEM, and the stretching direction;  $D(\alpha)$  is the orientation distribution function.

## 2.2. Shrinkage kinetics

To determine the electrospun mats shrinkage kinetics, the images of the mats immersed into ethanol were taken every 2 s by Logitech Webcam C925e using Webcam Surveyor 3.6.1. The initial size of each mat was either  $4 \times 4 \text{ cm}^2$ ,  $3 \times 3 \text{ cm}^2$  or  $2 \times 2 \text{ cm}^2$ . Sometimes the ethanol immersion of mats led to their rollup. Therefore, only those mats that remained flat during the whole shrinkage process were chosen for calculations. The linear sizes and areas of the mats were measured using the Fiji software. The same calculations were performed for the electrospun mats immersed into butanol.

## 2.3. Mechanical study

Mechanical studies of the PLA electrospun mats were performed using universal electromechanical test machine Autograph AGS-10 kNG (Shimadzu, Japan). The size of each sample stretched area was  $20 \times 5 \text{ mm}^2$ , the mat's thickness was in the range from 100  $\mu\text{m}$  to 200  $\mu\text{m}$ . Four types of tensile tests were carried out (Fig. 1): stretching of the electrospun PLA mats in air and ethanol, stretching of the PLA electrospun mats after the ethanol immersion (either fixed-ends or free-ends) and drying in Vacuum drying chamber (BINDER, USA) during 4 h at room temperature. All the tensile tests were carried out at an elongation rate of 5 mm/min. Also, the stress versus time dependence was recorded during the ethanol treatment of the fixed-ends samples. Experiments of each type were carried out at least three times.

## 2.4. Cell culturing

In order to provide better cell adhesion and attachment each PLA mat was incubated in 1 ml of 0.1 mg/ml poly-L-ornithine solution for half an hour at room temperature. Then specimens were rinsed with water three times and left for 2 h at room temperature for drying. After that, HaCaT human keratinocytes were seeded onto poly-L-ornithine-coated electrospun mats (20,000 cells/ml) and cultivated in complete growth medium DMEM (Paneco, Russia) with 10% fetal bovine serum (HyClone, United States), 4 mM L-glutamine (Paneco, Russia), and gentamicin (53  $\mu\text{g/ml}$ , Borisov Plant of Medical Preparations, Belarus) for 20 h.

## 2.5. Cell proliferation and viability tests

The assessment of proliferative activity was performed on 1, 3 and 5 days of experiment by counting cell numbers in 20 random microscopic fields of view after Hoechst 33258 and propidium iodide staining with the Fiji software. All specimens were investigated with 10x/0.25 lens of fluorescent microscope Axio Lab.A1 (Zeiss, Germany) using DS-F12 camera (Nikon, Japan).

## 2.6. Scanning electron microscopy (SEM)

For SEM examination HaCaT human keratinocytes were fixed with 2.5% glutaraldehyde in PBS for 2 h at room temperature, gradually dehydrated in ethanol and chemically dried with hexamethyldisilazane as described in [26]. Both electrospun mats and cells were covered by 10 nm gold palladium alloy using Sputter Coater Q150T (Quorum Technologies, UK). Mats and HaCaT human keratinocytes were characterized using a Zeiss Merlin microscope equipped with GEMINI II Electron Optics (Zeiss, Germany) at 1–3 kV accelerating voltage and 70–100 pA probe current. The average fiber diameter and the fiber orientation were calculated using plugin Diameter] in the Fiji software [27].

## 2.7. WAXS measurements

WAXS measurements were performed using a XeuSS SAXS/WAXS (Xenocs, France) machine coupled to a GeniX3D generator ( $\lambda = 1.54 \text{ \AA}$ ) for initial PLA, electrospun mats before and after 2, 10 and 30 min ethanol treatment either free- and fixed-ends. We also investigated the PLA mats stretched in air or ethanol with the elongation 40–60% and 100% respectively (Fig. 1). The air-stretched mats deformed non-uniformly via necking mechanism and ruptured; thus, WAXS analysis was carried out in near the rupture area. All the other samples were relatively uniform, so the examination points were chosen randomly. The calculation of the WAXS orientation factor for uniaxially stretched mats

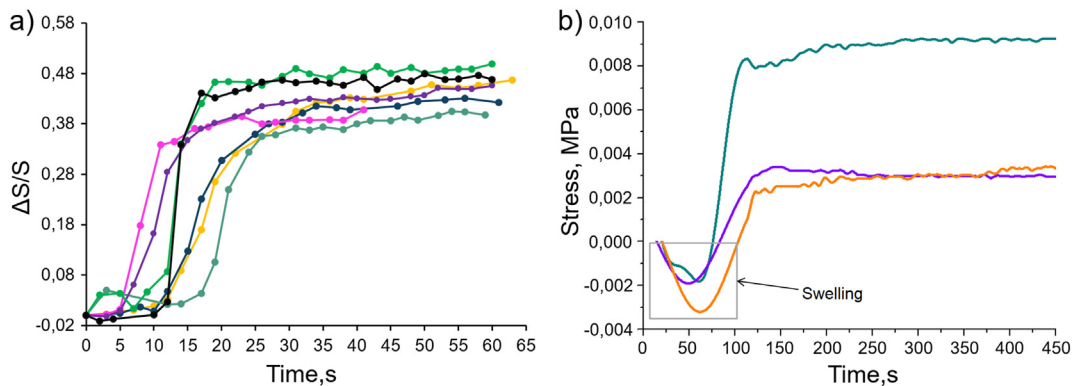


Fig. 2. Shrinkage kinetics of electrospun PLA mats investigated by a) controlling of mats area and b) recording of shrinkage force (stress). Each line on both graphs corresponds to an independent experiment. Slight differences between the lines can be associated with variations in mats thickness.

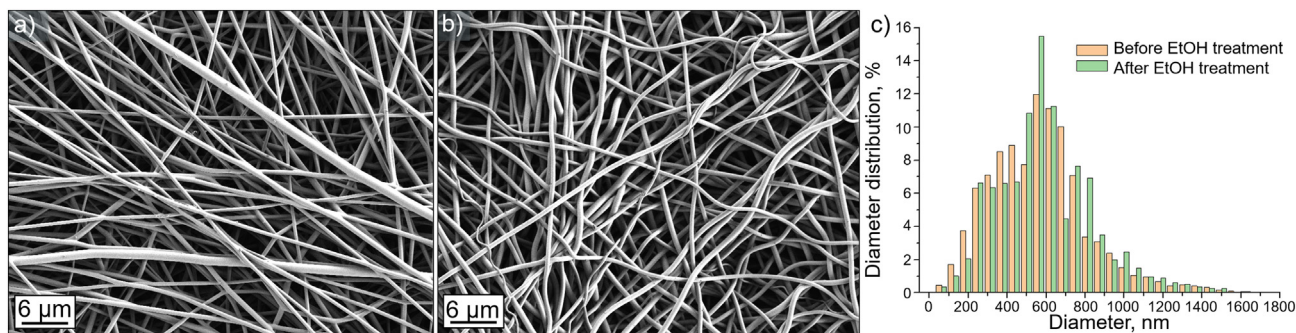


Fig. 3. SEM images of electrospun mats before (a) and after (b) ethanol treatment for 10 min. Distribution of the fibers diameters before and after ethanol treatment (c).

was performed using 2D WAXS data similarly to Eq. (1) and in line with the previous publications [25,28,29].

The 2D data were collected using a Rayonix HS170 CCD detector (pixel size  $132 \times 132 \mu\text{m}$ ) with the sample-to-detector distance of approximately 18 cm. The minimum projection method was used to reduce background noise. The modulus of the scattering vector was calibrated using several diffraction orders of silver behenate powder. Analysis of 2D-WAXS patterns was performed with the help of a home-made routine designed Igor Pro software (Wavemetrics Ltd.).

### 2.8. Statistical data processing

Data processing was done using Origin (OriginLab, USA). The measurement results presented in the text are shown as (Mean  $\pm$  SD) unless indicated otherwise.

## 3. Results and discussion

### 3.1. Mats characterization and shrinkage kinetics

Treatment of electrospun PLA mats in ethanol was accompanied by a rapid reduction in the size of the mats. The ethanol-induced shrinkage kinetics was characterized by the relative change of the mats area ( $\Delta S/S$ ) as a function of time (Fig. 2a). This kinetics had three distinct stages: ethanol penetration, rapid size reduction, and the plateau stage. These three stages were also observed when the PLA mats were treated with ethanol at constant size, and the mechanical stress was recorded (Fig. 2b).

The first process took about 15 s and was accompanied by swelling of the material which was confirmed by a decrease of stress (Fig. 2b). The second process reflected the effect of PLA mats area reduction from 35% to 55% and took no  $>30$  s. Then the shrinkage process reached the plateau, and the mats didn't decrease in size any further even after ethanol removal. Assuming that ethanol diffuses through the whole fiber volume and mean fiber radius ( $r$ ) is 500 nm (shown below) we calculated the diffusion coefficient ( $D_{et}$ ) of ethanol in PLA:

$$D_{et} \sim \frac{r^2}{t} \sim \frac{(500 \text{ nm})^2}{50 \text{ s}} \sim 5 \cdot 10^{-11} \frac{\text{cm}^2}{\text{s}},$$

$t$  – average time of first two processes (ethanol penetration and the rapid size reduction)

A similar shape of the shrinkage curve was observed for PLA mats in butanol. However, penetration and size reduction process in butanol took more time (Fig. S1) than in ethanol, which could be caused by a

$$\text{lower diffusion coefficient: } D_{but} \sim \frac{r^2}{t} \sim \frac{(500 \text{ nm})^2}{75 \text{ min}} \sim 6 \cdot 10^{-13} \frac{\text{cm}^2}{\text{s}}.$$

Shrinkage of the mats was accompanied by two morphological changes (Fig. 3): upon the ethanol treatment the fibers became crimped (Fig. 3b), and their mean diameter increased (Fig. 3c). The fiber diameters before (mean diameter = 570 nm, median = 560 nm, SD = 260 nm) and

after (mean diameter = 600 nm, median = 560 nm, SD = 260 nm) the ethanol treatment were significantly different according to Mann-Whitney test ( $p < 0,01$ ).

Both the fiber crimping and fiber diameter increase could be comprehended qualitatively if we assume relaxation of oriented PLA chains. Indeed, it is known that electrospinning often yields nanofibers containing oriented polymer chains [30,31]. Due to entropic reasons, the chain conformation tends to relax back to the isotropic coils when heated [32] or treated with a plasticizer. The effect of fiber crimping was more evident when the initial mats were aligned (Fig. S2).

### 3.2. Mechanical properties of electrospun mats before and after ethanol treatment

Ethanol was found to significantly modify the mechanical properties of electrospun mats. Ethanol made electrospun mats more stretchable (Fig. 4). The elongation at break for the electrospun mats in ethanol is approximately five times higher than the same value in air (Table 1), which provides evidence for the plasticization effect of ethanol to PLA (Fig. 4). The high elongation at break values were partially retained after drying of the ethanol treated mats (Table 1).

The mechanical properties were different when ethanol immersion was carried out in different conditions. In our mechanical experiments, different types of the electrospun mats were used such as the ones with free ends and fixed ends (Fig. 1). The fixed-ends mats did not shrink, and their fibers were not crimped unlike the free-end samples (Fig. S3). The two types of samples showed different values of Young's modulus. Thus, the samples with fixed ends gave higher Young's

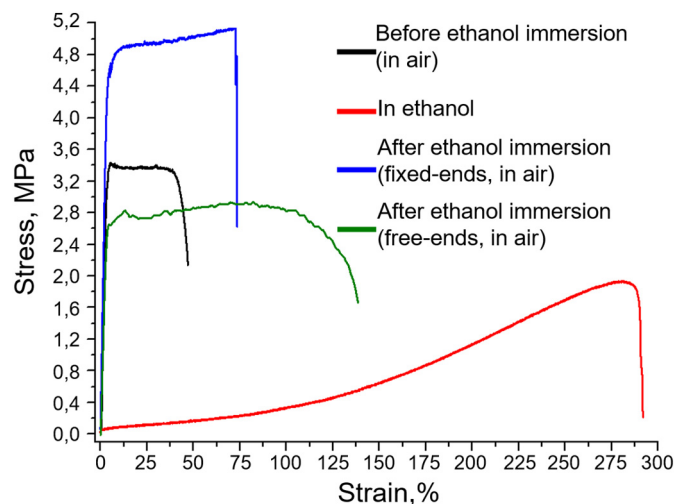


Fig. 4. Stress-strain curves of the electrospun mats. The duration of ethanol treatment (blue and green lines) was 5 min with subsequent drying. The stretching of the mats in ethanol (red line) was carried out immediately after ethanol addition.

**Table 1**Mechanical properties of the PLA electrospun mats. E -Young's modulus,  $\sigma$  - tensile strength,  $\epsilon$  - elongation at break.

	Before ethanol immersion (in air)	In ethanol	After ethanol immersion (fixed ends, in air)	After ethanol immersion (free ends, in air)
E, MPa	88 ± 22	0.8 ± 0.1	100 ± 22	57 ± 12
$\sigma$ , MPa	2.5 ± 0.9	1.6 ± 0.2	4.4 ± 0.9	2.6 ± 0.5
$\epsilon$ , %	49 ± 13	279 ± 13	110 ± 42	158 ± 43

modulus than the samples with free ends (Table 1). We have two explanations of this effect: an increase in crystallinity of the fixed-ends mats after the ethanol treatment and morphology-related changes in the elastic behavior of the free-ends mats. The first hypothesis did not find support because all the mats were amorphous, according to WAXS data (Fig. S4). Neither the free-ends mats nor the fixed-ends mats exhibited crystalline diffraction peaks upon 30 min of ethanol treatment, which is more than the shrinkage time. This result can be explained by the presence of 4.5% fraction D-isomer and also by the relatively short incubation time at RT. For example, effective crystallization (crystallinity degree ~ 30%) of electrospun PLLA mats took >5 h during annealing at higher temperature [14]. By contrast, the second hypothesis is likely to be correct because the crimped fibers can behave like springs: Young's modulus of a spring is lower than the modulus of a rod made of the same material. In other words, crimped fiber structure could give an additional mechanism of elastic deformation which resulted in a decrease of Young's modulus.

### 3.3. Mats stretching in ethanol

Highly aligned electrospun mats are often needed for biological applications as nerve guides [33,34], cardiovascular [35] and muscle [36] grafting materials and matrixes for contact guidance investigation [37,38]. Fabrication of aligned electrospun mats usually requires the use of special electrodes like pairs of blades [39], rotating drums and others [40]. However, it is often difficult to obtain highly aligned fibrous mats by electrospinning. The fundamental reason which randomizes the electrospun fibers alignment is the residual charge of the deposited fibers, which «spoils» the orientation of the newly generated fibers as the mat thickness increases [41]. Stretching of electrospun mats in a plasticizer allows solving this problem because the fibers align along the tensile direction entirely (Fig. 5). In this case, it is possible to align the mats without the use of special electrodes during electrospinning. According to distributions  $D(\alpha)$  of fibers orientation (Fig. 5e), the highest geometrical orientation factor  $f_g$  (0.92) corresponded to mats 100% stretched in ethanol. The orientation factors  $f_g$  (Eq. (1)) of mats aligned on blades, mats stretched in air and non-aligned ones were

0.71, 0.43 and 0.10 respectively (Fig. 5). Thus, alignment of electrospun mats by stretching in a plasticizer is more preferable than alignment using special collector electrode of two blades.

Moreover, we found that plasticizer protected fibers from multiple necking which appeared during stretching in air (Fig. 6). Multiple necking probably occurred during the plastic deformation process. There are two main competing processes during plastic deformation: orientation of the macromolecular chains and volume damage of the polymer [42]. If the polymer is in a viscoelastic state, the molecular orientation process dominates. Otherwise, the volume damaging process occurs which results in formation of voids inside the polymer and necking. In our case, the mobility of the macromolecular chains increased due to the lowering of the glass transition temperature of the PLA by adding the plasticizer. According to X-ray diffraction data (Fig. 7), the stretching of the electrospun PLA mats in ethanol led to the increase of orientation factor  $f_{WAXS}$  comparing to the air-stretched mat. Analyzing the azimuthal distribution of the amorphous halo, the orientation factor  $f_{WAXS}$  for electrospun PLA mats stretched in ethanol was 0.65, while the same parameter for the electrospun PLA mats stretched in air was close to 0.10. The deformation of the air-stretched mats ( $\epsilon$  in the range 40–60%) was lower than of those stretched in ethanol ( $\epsilon$ ~100%). However, WAXS analysis of the air-stretched mats was performed in the neck area near the rupture, where the local deformation was maximum (about 100–200%). Taking into account the values of the orientation factors  $f_{WAXS}$  (WAXS analysis) and  $f_g$  (SEM measurements), the molecular orientation factor  $f_m$  corresponding to an individual fiber can be calculated as  $f_m = f_{WAXS}/f_g$ . The decomposition of  $f_{WAXS}$  into the geometrical and molecular orientation factors is similar for the problem of successive molecular rotations [43]. Using the obtained  $f_m$  values, it can be concluded that stretching of the PLA mats in ethanol caused higher molecular orientation ( $f_m = 0.71$ ) than stretching in air ( $f_m = 0.23$ ).

In the experiments, we did not observe the damaging of the electrospun fibers stretched in ethanol (Fig. 6b). In contrast, the PLA fibers stretched in air displayed multiple necking (Fig. 6a). The same effect occurred during the electrospinning process because of the intense stretching of solidified nanofibers provoked by the strong electric field and the collector rotation [44].

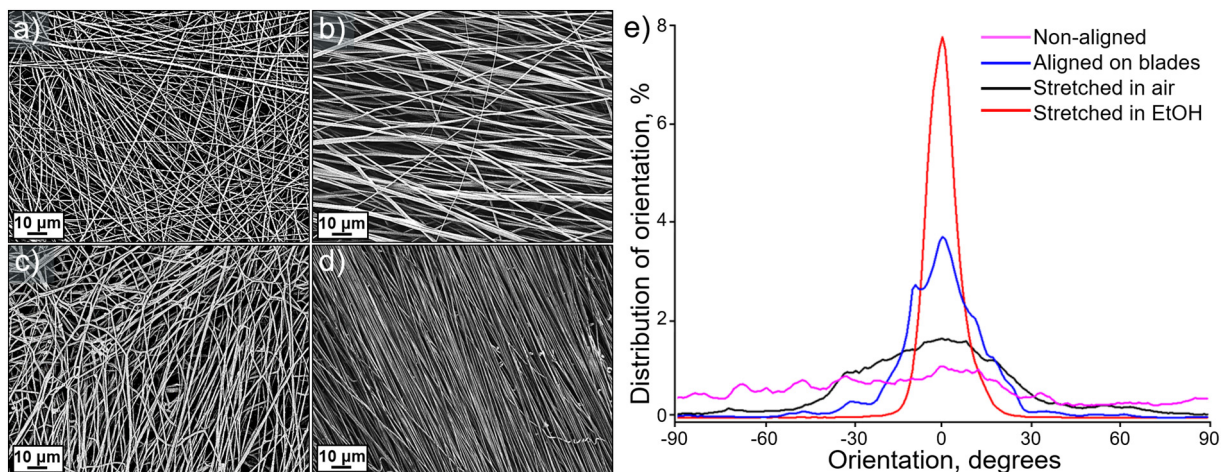


Fig. 5. Electrospun mats: (a) non-aligned, (b) aligned on blades, (c) 2 times stretched in air, (d) stretched in ethanol. Distributions  $D(\alpha)$  of fibers orientation (e).

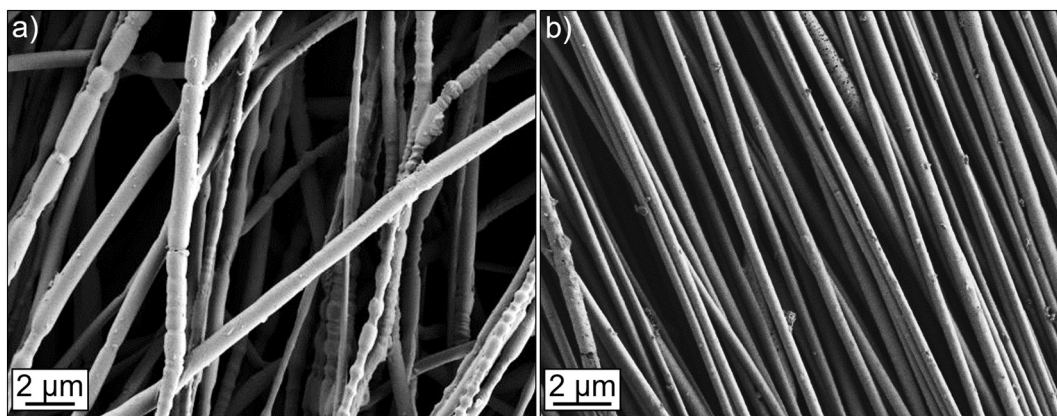


Fig. 6. Electrospun mats: (a) stretched in air, (b) stretched in ethanol.

### 3.4. Contact guidance of HaCaT human keratinocytes

Cell contact guidance is the changes in cell shape, adhesion and migration behavior induced by the substrate anisotropy [45,46]. Patterned substrates with grooves, pillars or aligned fibers are usually used for the contact guidance investigation [47,48]. In our previous works we demonstrated the possibility of HaCaT keratinocytes contact guidance on electrospun Nylon 6 and poly ( $\epsilon$ -caprolactone) mats aligned by the gap method [26,49,50]. In the present paper, we stretched the PLA mats in ethanol to align the fibers and induce the cell contact guidance.

We used aligned PLA mats with fibers of relatively large ( $1.8 \pm 0.8 \mu\text{m}$ ) and small ( $0.5 \pm 0.2 \mu\text{m}$ ) diameters for the HaCaT cells cultivation. Fig. 8 shows the cells grown on the large and small aligned fibers. For the quantitative analysis of cell aspect ratio (the ratio of the linear sizes of cell along the fibers and across them) we used only single cells, so that cell shape depended on the local morphology of the mats (fibers alignment, diameter, and pore size) only and the effect of cell-cell interactions on cell shape could be excluded. Mean aspect ratios of the cells grown on the mats consisting of the large and small fibers were  $3.4 \pm 1.7$  and  $3.0 \pm 1.6$ , respectively, and were not statistically different at 0.05 level. For comparison, the aspect ratio of HaCaT cells grown on the non-aligned electrospun PLA mats was significantly smaller –  $1.5 \pm 0.6$  (Fig. S5). This was in agreement with the previous data obtained for HaCaT cells grown on the non-aligned electrospun nylon mats [26]. Thus, stretching of the PLA mats in ethanol caused fiber alignment which was high enough to induce cell contact guidance.

Although both types of aligned mats induced contact guidance, its character varied. When cultured on the mats consisting of the  $1.8 \pm 0.8 \mu\text{m}$  fibers, the cells often leaned against one or two fibers and could migrate into the pores (Fig. S6). On the contrary, when cultured on the mats consisting of the  $0.5 \pm 0.2 \mu\text{m}$  fibers, the cells adhered to

a relatively large number of fibers ( $N > 10$ ) and did not penetrate the pores.

As described above, ethanol treatment of PLA mats changes their mechanical properties and morphology. Thus, alignment of mats by stretching them in ethanol may influence on proliferation of HaCaT keratinocytes. We compared the proliferation of HaCaT cells grown on the ethanol-stretched mats and the non-aligned ones. We counted the total number of cells and the dead cells grown on the aligned and random mats (the cells were stained with Hoechst and propidium iodide correspondingly). The percentage of the dead cells was  $<1\%$  throughout all 5 days of the experiment for both types of mats. Although the mean cell density was slightly larger for the aligned mats, the difference between the non-aligned and ethanol-stretched mats was not significantly different within each day. The mean cell density was growing slowly within the experiment (Fig. 9). Thus, we have demonstrated that the ethanol-stretched mats and non-aligned mats are non-cytotoxic and maintain cell proliferation at the same level.

### 4. Conclusion

Treatment of electrospun mats with a plasticizer can be used to tune their morphology in order to increase their biocompatibility [14,15]. The list of the polymer-plasticizer pairs is almost infinite, and it opens a massive list of opportunities for the properties adjustments of electrospun mats. Based on the literature data, ethanol treatment of electrospun mats could be accompanied by crystallization process. In order to avoid crystallization, for example for enhancement of the mat extensibility, we have selected PLA with a higher fraction of D-isomer (4.5%) than in the previous works reporting slow crystallization of PLA in absolute ethanol at RT.

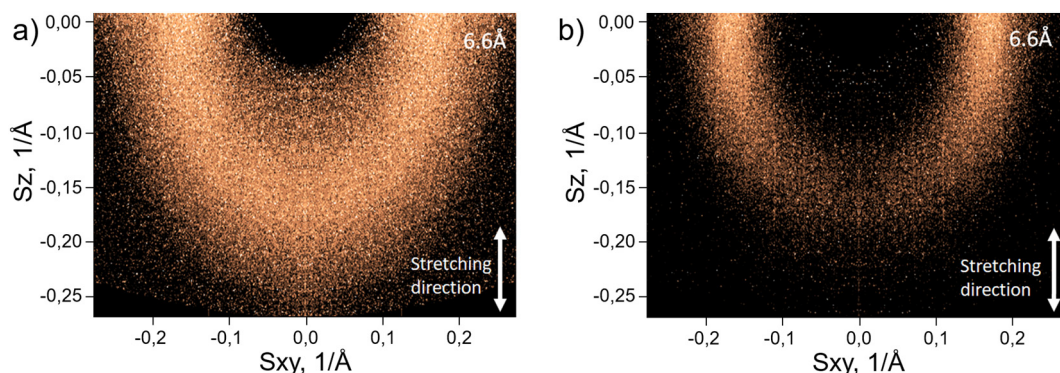


Fig. 7. 2D X-ray diffraction patterns of PLA mats stretched (a) in air and (b) in ethanol.

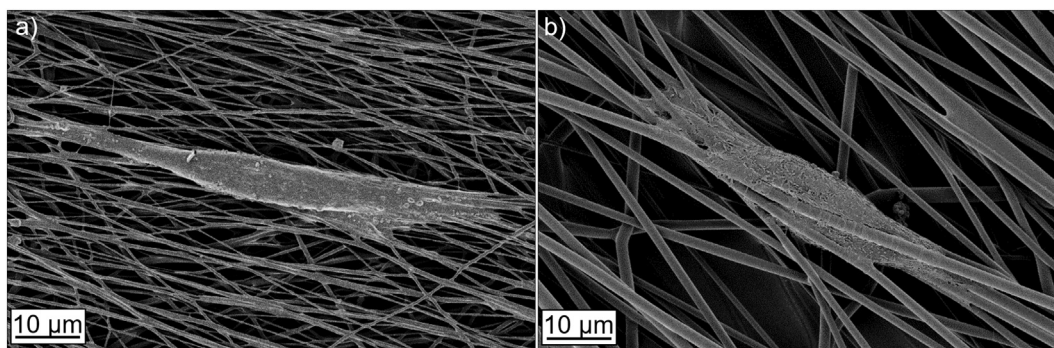


Fig. 8. HaCaT cells grown on the small (a) and large (b) aligned fibers.

The influence of ethanol on PLA electrospun mats was investigated at three levels: macro, micro, and molecular. At the macro level, the ethanol treatment of free-ends mats led to shrinkage within 50 s at room temperature. A similar effect was observed in butanol, but it took longer time (>20 min) due to the relatively slow diffusion of butanol into PLA. Ethanol made the PLA mats softer (decreased Young's modulus) and more stretchable. At the micro level, the ethanol treatment of the free-ends mats induced fibers crimping, while the fibers of the fixed-ends mats remained straight. Stretching of the PLA mats in ethanol did not lead to multiple necking (in contrast to stretching of the mats in air) and could be used to obtain highly aligned mats. At the molecular level, the intact and ethanol-treated PLA mats did not develop any crystallinity in the timeframe of the experiment according to WAXS. At the same time, WAXS showed enhanced molecular orientation in the mats stretched in ethanol.

The conformation of polymer chains in electrospun fibers is still relatively poorly described [30]. However, stretching of the electrospun PLA mats in ethanol or other plasticizers can be regarded as a novel simple method of producing highly aligned mats. This method yields higher fibers alignment than the gap method and does not require the rotating mandrel setup [40]. Such highly aligned mats can be used to induce cell contact guidance in biomedical applications. Contact guidance phenomenon can be used for tissue engineering because it might enhance the nerve regeneration process [51], provide formation of continuous muscle fibers [52] or induce alignment of cardiomyocytes for their synchronized contractility [53]. Our experiments with the HaCaT cells revealed high aspect ratio of the cells grown on the PLA mats stretched in ethanol and did not show differences in viability and proliferation rate of HaCaT cells grown on aligned and non-aligned mats. Further studies on single electrospun fibers using Raman micro-spectroscopy and diffraction techniques will provide more information on the micro-structure and chain conformation in such systems.

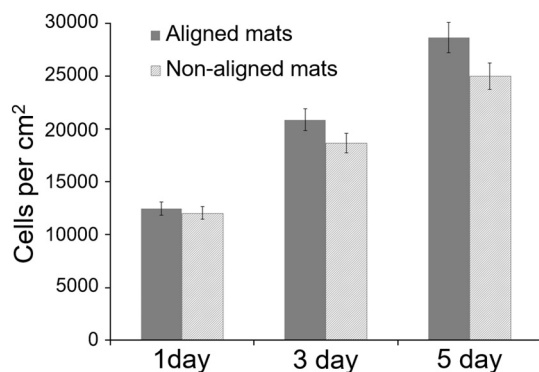


Fig. 9. Proliferation dynamics of HaCaT keratinocytes grown on the ethanol-stretched aligned PLA mats (fiber diameter  $d = 1.6 \pm 0.7 \mu\text{m}$ ) and the non-aligned mats ( $d = 1.6 \pm 0.7 \mu\text{m}$ ).

Supplementary data to this article can be found online at <https://doi.org/10.1016/j.matdes.2019.108061>.

### CRediT authorship contribution statement

**Elizaveta R. Pavlova:** Conceptualization, Methodology, Validation, Formal analysis, Investigation, Writing - original draft, Visualization. **Dmitry V. Bagrov:** Investigation, Data curation, Writing - original draft, Writing - review & editing, Supervision, Project administration. **Kristina Z. Monakhova:** Investigation. **Alexey A. Piryazev:** Investigation. **Anastasia I. Sokolova:** Investigation, Writing - review & editing. **Dimitri A. Ivanov:** Conceptualization, Writing - review & editing, Supervision. **Dmitry V. Klinov:** Conceptualization, Resources, Supervision, Project administration, Funding acquisition.

### Acknowledgment

Our research was supported by the Russian Science Foundation (grant № 17-75-30064). WAXS analysis was performed in accordance with state task № 0074-2019-0014 of Russian Academy of Sciences.

### Data availability

The raw/processed data required to reproduce these findings cannot be shared at this time due to time limitations.

### References

- [1] Y. Zhao, J. Gong, C. Niu, Z. Wei, J. Shi, G. Li, Y. Yang, H. Wang, A new electrospun graphene-silk fibroin composite scaffolds for guiding Schwann cells, *J. Biomater. Sci. Polym. Ed.* (2017) <https://doi.org/10.1080/09205063.2017.1386835>.
- [2] M. Leino, C. Astrand, N. Hughes-Brittain, B. Robb, R. McKean, V. Chotteau, Human embryonic stem cell dispersion in electrospun PCL fiber scaffolds by coating with laminin-521 and E-cadherin-Fc, *J. Biomed. Mater. Res. - Part B Appl. Biomater.* (2018) <https://doi.org/10.1002/jbm.b.33928>.
- [3] M. Sheikholeslam, M.E.E. Wright, M.G. Jeschke, S. Amini-Nik, Biomaterials for skin substitutes, *Adv. Healthc. Mater.* 7 (2018) 1–20, <https://doi.org/10.1002/adhm.201700897>.
- [4] F. Batool, D.-N. Morand, L. Thomas, I.M. Bugueno, J. Aragon, S. Irusta, L. Keller, N. Benkirane-Jessel, H. Tenenbaum, O. Huck, Synthesis of a novel electrospun polycaprolactone scaffold functionalized with ibuprofen for periodontal regeneration: an in vitro and in vivo study, *Mater. (Basel, Switzerland)* 11 (2018) <https://doi.org/10.3390/ma11040580>.
- [5] M. Zhu, J. Han, F. Wang, W. Shao, R. Xiong, Q. Zhang, H. Pan, Y. Yang, S.K. Samal, F. Zhang, C. Huang, Electrospun nanofibers membranes for effective air filtration, *Macromol. Mater. Eng.* 302 (2017) 1–27, <https://doi.org/10.1002/mame.201600353>.
- [6] F. Yalcinkaya, J. Hruza, Effect of laminating pressure on polymeric multilayer nanofibrous membranes for liquid filtration, *Nanomaterials* (2018) <https://doi.org/10.3390/nano8050272>.
- [7] H. Zhu, S. Qiu, W. Jiang, D. Wu, C. Zhang, Evaluation of electrospun polyvinyl chloride/polystyrene fibers as sorbent materials for oil spill cleanup, *Environ. Sci. Technol.* 45 (2011) 4527–4531, <https://doi.org/10.1021/es2002343>.
- [8] A. Celebioglu, F. Topuz, T. Uyar, Water-insoluble hydrophilic electrospun fibrous mat of cyclodextrin-epichlorohydrin polymer as highly effective sorbent, *ACS Appl. Polym. Mater.* (2019) <https://doi.org/10.1021/acscapm.8b00034>.

- [9] A. Kakoria, S. Sinha-Ray, A review on biopolymer-based fibers via electrospinning and solution blowing and their applications, *Fibers* (2018) <https://doi.org/10.3390/fib6030045>.
- [10] C. Zhang, F. Feng, H. Zhang, Emulsion electrospinning: fundamentals, food applications and prospects, *Trends Food Sci. Technol.* (2018) <https://doi.org/10.1016/j.tifs.2018.08.005>.
- [11] J.B. Lee, Y.-G. Ko, D. Cho, W.H. Park, B.N. Kim, B.C. Lee, I.-K. Kang, O.H. Kwon, Modification of PLGA nanofibrous mats by electron beam irradiation for soft tissue regeneration, *J. Nanomater.* (2015) <https://doi.org/10.1155/2015/295807>.
- [12] X. Wang, K. Zhang, M. Zhu, B.S. Hsiao, B. Chu, Enhanced mechanical performance of self-bundled electrospun fiber yarns via post-treatments, *Macromol. Rapid Commun.* (2008) <https://doi.org/10.1002/marc.200700873>.
- [13] E. Storti, O. Jankovský, P. Colombo, C.G. Aneziris, Effect of heat treatment conditions on magnesium borate fibers prepared via electrospinning, *J. Eur. Ceram. Soc.* (2018) <https://doi.org/10.1016/j.jeurceramsoc.2018.04.050>.
- [14] C. Gualandi, M. Govoni, L. Foroni, S. Valente, M. Bianchi, E. Giordano, G. Pasquinielli, F. Biscarini, M.L. Focarete, Ethanol disinfection affects physical properties and cell response of electrospun poly(L-lactic acid) scaffolds, *Eur. Polym. J.* 48 (2012) 2008–2018, <https://doi.org/10.1016/j.eurpolymj.2012.09.016>.
- [15] W. Liu, J. Lipner, C.H. Moran, L. Feng, X. Li, S. Thomopoulos, Y. Xia, Generation of electrospun nanofibers with controllable degrees of crimping through a simple, plasticizer-based treatment, *Adv. Mater.* 27 (2015) 2583–2588, <https://doi.org/10.1002/adma.201500329>.
- [16] D.C. Surrao, J.W.S. Hayami, S.D. Waldman, B.G. Amsden, Self-crimping, biodegradable, electrospun polymer microfibers, *Biomacromolecules* 11 (2010) 3624–3629, <https://doi.org/10.1021/bm101078c>.
- [17] D.C. Surrao, S.D. Waldman, B.G. Amsden, Biomimetic poly(lactide) based fibrous scaffolds for ligament tissue engineering, *Acta Biomater.* 8 (2012) 3997–4006, <https://doi.org/10.1016/j.actbio.2012.07.012>.
- [18] F. Chen, J.W.S. Hayami, B.G. Amsden, Electrospun poly(L-lactide-co -acryloyl carbonate) fiber scaffolds with a mechanically stable crimp structure for ligament tissue engineering, *Biomacromolecules* 15 (2014) 1593–1601, <https://doi.org/10.1021/bm401813j>.
- [19] P.-H.G. Chao, Crimped electrospun fibers for tissue engineering, *Methods Mol. Biol.* (2018) [https://doi.org/10.1007/978-1-4939-7741-3\\_12](https://doi.org/10.1007/978-1-4939-7741-3_12).
- [20] C. Ru, F. Wang, M. Pang, L. Sun, R. Chen, Y. Sun, Suspended, shrinkage-free, electrospun PLGA nanofibrous scaffold for skin tissue engineering, *ACS Appl. Mater. Interfaces* (2015) <https://doi.org/10.1021/acsami.5b01953>.
- [21] P.-H.G. Chao, H.-Y. Hsu, H.-Y. Tseng, Electrospun microcrimped fibers with nonlinear mechanical properties enhance ligament fibroblast phenotype, *Biofabrication* (2014) <https://doi.org/10.1088/1758-5082/6/3/035008>.
- [22] A. Sensini, L. Cristofolini, Biofabrication of electrospun scaffolds for the regeneration of tendons and ligaments, *Materials* (Basel) (2018) <https://doi.org/10.3390/ma11101963>.
- [23] J. Horakova, P. Mikes, A. Saman, V. Jencova, A. Klapstova, T. Svarcova, M. Ackermann, V. Novotny, T. Suchy, D. Lukas, The effect of ethylene oxide sterilization on electrospun vascular grafts made from biodegradable polyesters, *Mater. Sci. Eng. C* (2018) <https://doi.org/10.1016/j.msec.2018.06.041>.
- [24] V.N. Morozov, A.Y. Mikhchev, Water-soluble polyvinylpyrrolidone nanofibers manufactured by electro-spray-neutralization technique, *J. Memb. Sci.* 403–404 (2012) 110–120, <https://doi.org/10.1016/j.memsci.2012.02.028>.
- [25] M. Pick, R. Lovell, A.H. Windle, X-ray measurement of chain orientation in non-crystalline polymers, *Polym. (United Kingdom)* (1980) [https://doi.org/10.1016/0032-3861\(80\)90031-2](https://doi.org/10.1016/0032-3861(80)90031-2).
- [26] A.I. Sokolova, E.R. Pavlova, Y.V. Khramova, D.V. Klinov, K.V. Shaitan, D.V. Bagrov, Imaging human keratinocytes grown on electrospun mats by scanning electron microscopy, *Microsc. Res. Tech.* (2019) 2010–2015, <https://doi.org/10.1002/jemt.23198>.
- [27] N.A. Hotaling, K. Bharti, H. Kriel, C.G. Simon, DiameterJ: a validated open source nanofiber diameter measurement tool, *Biomaterials* 61 (2015) 327–338, <https://doi.org/10.1016/j.biomaterials.2015.05.015>.
- [28] G. Colombe, S. Gree, O. Lhost, M. Dupire, M. Rosenthal, D.A. Ivanov, Correlation between mechanical properties and orientation of the crystalline and mesomorphic phases in isotactic polypropylene fibers, *Polymer (Guildf)* 52 (2011) 5630–5643, <https://doi.org/10.1016/j.polymer.2011.09.035>.
- [29] E.M. Khar'kova, D.I. Mendeleev, V.A. Aulov, B.F. Shklyaruk, V.A. Gerasin, A.A. Pirayev, A.E. Antipov, Nanocomposites and high modulus fibers based on ultrahigh molecular weight polyethylene and silicates: synthesis, structure, and properties, *Polym. Sci. Ser. A* (2014) <https://doi.org/10.1134/S0965545X14010052>.
- [30] M. Richard-Lacroix, C. Pellerin, Molecular orientation in electrospun fibers: from mats to single fibers, *Macromolecules* 46 (2013) 9473–9493, <https://doi.org/10.1021/ma401681m>.
- [31] L.M. Bellan, H.G. Craighead, Molecular orientation in individual electrospun nanofibers measured via polarized Raman spectroscopy, *Polymer (Guildf)* 49 (2008) 3125–3129, <https://doi.org/10.1016/j.polymer.2008.04.061>.
- [32] Q. Ma, M. Pyda, B. Mao, P. Cebe, Relationship between the rigid amorphous phase and mesophase in electrospun fibers, *Polymer (Guildf)* 54 (2013) 2544–2554, <https://doi.org/10.1016/j.polymer.2013.03.019>.
- [33] H.K. Frost, T. Andersson, S. Johansson, U. Englund-Johansson, P. Ekström, L.B. Dahlin, F. Johansson, Electrospun nerve guide conduits have the potential to bridge peripheral nerve injuries *In Vivo, Sci. Rep.* (2018) 1–13, <https://doi.org/10.1038/s41598-018-34699-8>.
- [34] H.B. Wang, M.E. Mullins, J.M. Cregg, A. Hurtado, M. Oudega, M.T. Trombley, R.J. Gilbert, Creation of highly aligned electrospun poly-L-lactic acid fibers for nerve regeneration applications, *J. Neural Eng.* 6 (2009) <https://doi.org/10.1088/1741-2560/6/1/016001>.
- [35] K.K. Sankaran, U.M. Krishnan, S. Sethurama, Axially aligned 3D nanofibrous grafts of PLA – PCL for small diameter cardiovascular applications, *J. Biomater. Sci.* (2014) 37–41, <https://doi.org/10.1080/09205063.2014.950505>.
- [36] K. Aviss, J. Gough, S. Downes, Aligned electrospun polymer fibres for skeletal muscle regeneration, *Eur. Cells Mater.* 19 (2010) 193–204, <https://doi.org/10.22203/ecm.v019a19>.
- [37] A.K. Gaharwar, M. Nikkha, S. Sant, A. Khademhosseini, Anisotropic poly (glycerol sebacate)-poly ( $\epsilon$ -caprolactone) electrospun fibers promote endothelial cell guidance, *Biofabrication* 7 (2015) <https://doi.org/10.1088/1758-5090/7/1/015001>.
- [38] S. Shang, F. Yang, X. Cheng, X.F. Walboomers, J.A. Jansen, The effect of electrospun fibre alignment on the behaviour of rat periodontal ligament cells, *Eur. Cells Mater.* 19 (2010) 180–192.
- [39] T. Lei, Z. Xu, X. Cai, L. Xu, D. Sun, New insight into gap electrospinning: toward meter-long aligned nanofibers, *Langmuir* (2018) <https://doi.org/10.1021/acs.langmuir.8b03114>.
- [40] M.M.L. Arras, C. Grasl, H. Bergmeister, H. Schima, Electrospinning of aligned fibers with adjustable orientation using auxiliary electrodes, *Sci. Technol. Adv. Mater.* 13 (2012) 1–8, <https://doi.org/10.1088/1468-6996/13/3/035008>.
- [41] L. Liu, Y.A. Dzenis, Analysis of the effects of the residual charge and gap size on electrospun nanofiber alignment in a gap method, *Nanotechnology* 19 (2008) <https://doi.org/10.1088/0957-4484/19/35/355307>.
- [42] M. Ponçot, F. Addiego, A. Dahoun, True intrinsic mechanical behaviour of semi-crystalline and amorphous polymers: influences of volume deformation and cavities shape, *Int. J. Plast.* 40 (2013) 126–139, <https://doi.org/10.1016/j.iplasp.2012.07.007>.
- [43] B. Corry, D. Jayatilaka, B. Martinac, P. Rigby, Determination of the orientational distribution and orientation factor for transfer between membrane-bound fluorophores using a confocal microscope, *Biophys. J.* (2006) <https://doi.org/10.1529/biophysj.106.080713>.
- [44] E. Zussman, D. Rittel, A.L. Yarin, Failure modes of electrospun nanofibers failure modes of electrospun nanofibers, *Appl. Phys. Lett.* 3958 (2003) 14–17, <https://doi.org/10.1063/1.1579125>.
- [45] C.J. Bettinger, R. Langer, J.T. Borenstein, Engineering substrate topography at the micro- and nanoscale to control cell function, *Angew. Chemie - Int. Ed.* (2009) <https://doi.org/10.1002/anie.200805179>.
- [46] D.H. Kim, P.P. Provenzano, C.L. Smith, A. Levchenko, Matrix nanotopography as a regulator of cell function, *J. Cell Biol.* (2012) <https://doi.org/10.1083/jcb.201108062>.
- [47] E. Jacchetti, C. Di Rienzo, S. Meucci, F. Nocchi, F. Beltram, M. Cecchini, Wharton's jelly human mesenchymal stem cell contact guidance by noisy nanotopographies, *Sci. Rep.* (2014) <https://doi.org/10.1038/srep03830>.
- [48] D. Kai, M.P. Prabhakaran, G. Jin, S. Ramakrishna, Guided orientation of cardiomyocytes on electrospun aligned nanofibers for cardiac tissue engineering, *J. Biomed. Mater. Res. - Part B Appl. Biomater.* (2011) <https://doi.org/10.1002/jbmb.b31862>.
- [49] E.R. Pavlova, D.V. Bagrov, Y.V. Khramova, D.V. Klinov, K.V. Shaitan, Nuclei deformation in HaCaT keratinocytes cultivated on aligned fibrous substrates, *Moscow Univ. Biol. Sci. Bull.* 72 (2017) 85–90, <https://doi.org/10.3103/S0096392517020043>.
- [50] A.I. Sokolova, E.R. Pavlova, Y.V. Khramova, D.V. Bagrov, D.V. Klinov, K.V. Shaitan, Application of fluorescence and scanning electron microscopy for the investigation of cell contact guidance, *AIP Conf. Proc.* 020004 (2019) 020004, <https://doi.org/10.1063/1.5087660>.
- [51] L. Ghasemi-Mobarakeh, M.P. Prabhakaran, M. Morshed, M.-H. Nasr-Esfahani, S. Ramakrishna, Electrospun poly( $\epsilon$ -caprolactone)/gelatin nanofibrous scaffolds for nerve tissue engineering, *Biomaterials* 29 (2008) 4532–4539, <https://doi.org/10.1016/j.biomaterials.2008.08.007>.
- [52] S.A. Riboldi, M. Sampaolese, P. Neuenschwander, G. Cossu, S. Mantero, Electrospun degradable polyesterurethane membranes: potential scaffolds for skeletal muscle tissue engineering, *Biomaterials* 26 (2005) 4606–4615, <https://doi.org/10.1016/j.biomaterials.2004.11.035>.
- [53] H.G. Şenel Ayaz, A. Perets, H. Ayaz, K.D. Gilroy, M. Govindaraj, D. Brookstein, P.I. Lelkes, Textile-templated electrospun anisotropic scaffolds for regenerative cardiac tissue engineering, *Biomaterials* 35 (2014) 8540–8552, <https://doi.org/10.1016/j.biomaterials.2014.06.029>.